21 January 2000

ELSEVIER

Chemical Physics Letters 316 (2000) 425–432

CHEMICAL PHYSICS LETTERS

www.elsevier.nl/locate/cplett

Isotope effects in the deactivation of $O(^1D)$ atoms by XCl and XF (X = H,D)

A.I. Chichinin *

Institute of Chemical Kinetics and Combustion, 630090 Novosibirsk, Russian Federation

Received 4 November 1999; in final form 17 November 1999

Abstract

The method of time-resolved laser magnetic resonance (LMR) was used to study the deactivation of $O(^1D)$ by HCl, DCl, HF, and DF at room temperature. For $O(^1D) + XF(X = H, D)$, the effect of deuteration on the rates of physical quenching and chemical reaction was negligible. For $O(^1D) + XCl$, no essential isotope effect on the deactivation rate, on the Cl + OX reaction channel probability, and on the relative quantum yields of spin–orbit excited $Cl(^2P_{1/2})$ atoms was found. While the formation of H + ClO is found to account for 0.18 ± 0.04 of the deactivation rate, in the deuterated case this channel was negligible (< 0.03).

1. Introduction

The collisional deactivation of excited oxygen atoms O^* ($\equiv O(2^1D_2)$) by halogen halides has been studied extensively both because of its contribution to atmospheric chemistry [1] and also due to its importance in molecular reaction dynamics [2–5]. In the present Letter, which extends our earlier LMR studies [6–8], we present a study of the isotope effect on the deactivation of O^* by XCl and XF at room temperature. The reactions of O^* with HCl can proceed via three competing pathways,

$$O^* + HCl \rightarrow Cl + OH, \quad \Delta H = -44.4\,\text{kcal/mol}, \tag{1a}$$

$$\rightarrow H + ClO, \quad \Delta H = -6.3\,\text{kcal/mol}, \tag{1b}$$

$$\rightarrow O + HCl, \quad \Delta H = -45.4\,\text{kcal/mol}. \tag{1c}$$

While kinetic data for this reaction are reported in the literature, relatively little is known about its deuterated analog,

$$O^* + DCl \rightarrow Cl + OD, \tag{2a}$$

$$\rightarrow D + ClO, \tag{2b}$$

$$\rightarrow O + DCl. \tag{2c}$$

To date there exists only one experimental study of deactivation of O^* by DCl at high collisional energy (~ 7.6 kcal/mol) carried out by Matsumi et al. by the REMPI technique [9]. By monitoring Cl, H, and D atoms the branching ratios for the reactive channels have been directly measured, and a strong isotope effect ($k_{1b}/k_{1a} \approx 2.7\, k_{2b}/k_{2a}$) was found. This isotope effect is considerably greater than would be predicted from statistical theory. This discrepancy has stimulated the present study.

In order to refine the understanding of such systems, we have also investigated the reaction

$$O^* + HF \rightarrow F + OH, \tag{3a}$$

$$\rightarrow O + HF, \tag{3b}$$

* E-mail: chichini@ns.kinetics.ncs.ru

0009-2614/00/$ - see front matter
PII: S0009-2614(99)01325-1

and its deuterated analog,

$$O^* + DF \rightarrow F + OD, \quad (4a)$$

$$\rightarrow O + DF. \quad (4b)$$

The present work was also undertaken to study the relative quantum yields of spin–orbit excited chlorine atoms Cl^* ($\equiv Cl(^2P_{1/2})$) in reactions (1a) and (2a). Note that this isotope effect has been measured only at high collisional energy [9].

2. Experimental

The experimental arrangement used in the present work has been described previously [6,7]. Briefly, it involves time-resolved LMR detection of Cl atoms and FO radicals. These species were produced in chemical reactions initiated by the photolysis of O_3. The photolysis source was a KrF laser (ELI-94, 248 nm, 50 mJ/pulse, 1 cm^2 cross-section, at 3 Hz). Gas mixtures containing O_3, halogen halides, SF_6, Cl_2, and He were pumped through a Pyrex cell (15 cm long, 1.9 cm i.d.) at a rate of 3 m/s. Typical experimental conditions were: $[O_3] = 3.5 \times 10^{13}$, $[SF_6] = 2.5 \times 10^{15}$, $[XCl] = (1–3000) \times 10^{13}$, $[He] = 3.0 \times 10^{17}$, all in units cm^{-3}; as indicated later, in some experiments SF_6 was absent.

The cell was inserted into the cavity of a CO_2 laser and was subjected to oscillating (150 kHz, amplitude 40 G) and constant magnetic fields. The unfocused excimer laser beam was aligned to the direction of the IR beam at an angle of $\sim 3°$. The outlet CO_2 laser radiation went to a GeHg photoresistor, cooled by solid N_2 (53 K). The signal of the photoresistor was detected by a lock-in amplifier, digitized, and transferred to a computer.

Cl atoms were detected by fine-structure $^2P_{1/2} \leftarrow {}^2P_{3/2}$ absorption using the 11 P(36) line of a $^{13}CO_2$ laser (882.287 cm^{-1}) at 3.57 kG [10,11]. FO radicals were detected on v, J:1, 1.5 ← 0, 1.5 transition using the 9P(34) line of a $^{12}CO_2$ laser (1033.488 cm^{-1}) at 1.002 kG [12,13]. In both cases $E \perp B$ polarization was used.

The main experimental problems were connected with premature reactions of HF and DF and with H ↔ D exchange. A greaseless flow system was used; gas flow lines exterior to the cell were constructed of either stainless steel or copper with clamped Teflon O-ring joints; the cell was constructed of Teflon entirely. All the gas handling and storage components were passivated by F_2 at ~ 1 atm during several months before experiments. To reduce the H ↔ D exchange problem, one flow line was used for deuterium containing gases only, it was purged by DCl for a period of several weeks before the experiments; the second line was used for H-containing gases only.

Cl_2 and HCl were prepared by standard techniques [14] and contained $< 1\%$ of impurities. The deuterated gases DF and DCl were prepared in reactions $CaF_2 + D_2SO_4$ and $PCl_3 + D_2O$, respectively. Passivation of mass spectrometer lines by deuterated gases was not complete, hence the measured [H]/[D] ratio was found to be < 0.1; presumably it is ~ 0.01. O_3 was obtained just before experiments by a 10 kV – 50 Hz AC discharge in a vessel with O_2 cooled by liquid N_2. The purities of commercial HF, SF_6, and He were 99%, $> 99\%$, and $> 99.999\%$, respectively.

3. Results

3.1. Designations

The following designations are introduced in this Letter. $\boldsymbol{k}(M_1, M_2, \ldots) \equiv k_{M_1}[M_1] + k_{M_2}[M_2] + \ldots$ denotes the pseudo-first-order rate constant for deactivation of O^* by $M_1, M_2, \ldots$ molecules; k_{M_i} is the rate constant for deactivation of O^* by M_i molecules. S_{Cl} and S_{FO} are the maximum amplitude of the LMR signal of Cl atoms and FO radicals, respectively. β_1 and β_2 denote the relative yield of Cl^* atoms ($\equiv [Cl(^2P_{1/2})]/([Cl(^2P_{1/2})] + [Cl(^2P_{3/2})]$) in reactions (1a) and (2a), respectively. The results on $O^* + XCl$, XF systems obtained in this study are summarized in Tables 1 and 2, along with the literature data.

3.2. Total quenching of O^* by DCl

The method for determination of the rate constants for deactivation of O^* by chlorides has been described previously, when it was used to determine

Table 1
Rate constants for deactivation of O^* by M molecules at $T = 300$ K

M	Products	Rate constant (10^{-11} cm^3/s)	Refs.
HF	([a])	5.1 ± 1.0	[7]
	F + OH	1.5 ± 0.3	[7]
	O + HF	3.6 ± 0.7[c]	[7]
DF	([a])	5.1 ± 2.0	([b])
	F + OD	1.5 ± 0.5	([b])
	O + DF	3.6 ± 2.0[c]	([b])
HCl	([a])	15 ± 1	[6,17–19], b)
	Cl + OH	10 ± 2	[6,18], ([b])
	H + OCl	3.6 ± 1	[18], ([b])
	O + HCl	1.35 ± 0.8	[18]
DCl	([a])	14.5 ± 2	([b])
	Cl + OD	10.6 ± 2	([b])
	D + DCl	< 0.6	([b])
	O + OCl	3.6 ± 1.4[d]	([b])

[a] Overall deactivation of O^*.
[b] This Letter.
[c] Calculated by difference as $k_{ib} = k_i - k_{ia}$, $i = 3, 4$.
[d] Calculated by difference as $k_{2c} = k_2 - k_{2a} - k_{2b}$.

k_1 [6]. In the present study the same method is used to measure k_2.

In the experiments of this kind [DCl] was varied, while $[O_3]$, $[SF_6]$, and [He] were kept constant; the time of Cl signal rise was measured. The photolysis of O_3 by radiation with $\lambda = 248$ nm yields dominantly O^* atoms [15]. The removal of these atoms is first order, with a decay time given by $1/\tau = \boldsymbol{k}(\mathrm{DCl}, \mathrm{O_3}, \mathrm{SF6}, \mathrm{He})$. After photolysis pulse, Cl atoms are produced only by the $O^* + DCl$ reaction. Under experimental conditions used in the present study secondary removal or formation of Cl is unimportant. Hence, the Cl first-order appearance rate should be equal to the O^* first-order disappearance rate.

The time-resolved LMR signal of Cl atoms displays a fast rise followed by a slow decay. The slow decay component is due to reaction $Cl + O_3$ and the diffusion of Cl from the probe volume. Least-squares fits of the signals to biexponential expression give the rise time τ (10–100 μs) and fall time τ_d (~ 2 ms). Plot of $1/\tau$ vs. [DCl] is presented in Fig. 1. The slope of the least-squares line yields the rate

Table 2
Channel branching ratios for $O^* + XCl$, XF systems

Reagents	Conditions	Branching ratio[a]	Ref.
$O^* + HCl$	$T = 300$ K	$P(O) = 0.09 \pm 0.05$	[18]
	$T = 300$ K	$P(H) = 0.24 \pm 0.05$	[18]
	$T = 300$ K	$P(Cl) = 0.67 \pm 0.10$	[18]
	$E_{col} = 7.6$ kcal/mol	$P(O) \approx 0.053 \pm 0.015$	[20]
	$E_{col} = 12.2$ kcal/mol	$P(H)/P(Cl) \geq 0.34 \pm 0.10$	[21]
	$E_{col} = 7.6$ kcal/mol	$P(H)/P(Cl) = 0.24 \pm 0.06$	[9]
	$T = 300$ K	$P(Cl) = 0.63 \pm 0.10$	[6]
	$T = 300$ K	$P(H)/P(Cl) = 0.28 \pm 0.05$	([b])
	$T = 300$ K	$P(O) = 0.19 \pm 0.13$[c]	([b])
	$T = 300$ K	$P(H) = 0.18 \pm 0.4$[d]	([b])
$O^* + DCl$	$E_{col} = 7.7$ kcal/mol	$P(D)/P(Cl) = 0.09 \pm 0.02$	[9]
	$T = 300$ K	$P(Cl) = 0.73 \pm 0.08$	([b])
	$T = 300$ K	$P(D)/P(Cl) < 0.04$	([b])
	$T = 300$ K	$P(O) = 0.25 \pm 0.09$[c]	([b])
	$T = 300$ K	$P(D) < 0.04$[d]	([b])
$O^* + HF$	$T = 300$ K	$P(F) = 0.30 \pm 0.02$	[7]
$O^* + DF$	$T = 300$ K	$P(F) = 0.30 \pm 0.05$	([b])

[a] $P(A)$ is the probability of the A atom separation channel, for $O^* + AB$ we have $P(O) + P(A) + P(B) = 1$. The quoted error bounds reflect 2σ.
[b] This Letter.
[c] Calculated by difference as $P(O) = 1 - P(Cl) \times [1 + P(X)/P(Cl)]$.
[d] Calculated as $P(X) = P(Cl) \times P(X)/P(Cl)$.

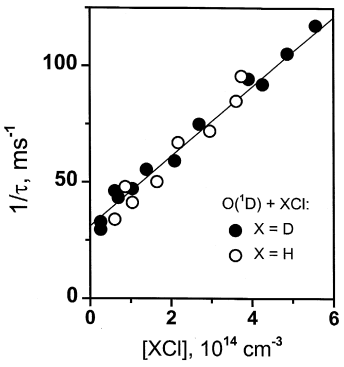

Fig. 1. Reciprocal rise time of Cl atoms signal, $1/\tau$, vs. [XCl]. LMR signals of Cl atoms were obtained by the photolysis of O_3 followed by the $O(^1D)+XCl$ reaction. The $O(^1D)+XCl$ deactivation rate constant is the slope of the line, the intercept of corresponds mainly to deactivation of $O(^1D)$ by O_3. Typical experimental conditions were: $[O_3]=10^{13}$, $[SF_6]=2.5\times10^{15}$, $[He]=3\times10^{17}$, all in units of cm^{-3}.

constant k_2, see Table 1. For comparison, the same measurements have been done for $O^* + HCl$. The results are presented in Fig. 1. The figure confirms that, within experimental error, the rate constants k_1 and k_2 are equal.

To deactivate spin–orbitally excited atoms Cl^* produced in reactions (1a) and (2a) [6,9], considerable amount of SF_6 was added. SF_6 molecule is an effective quencher of Cl^* atoms, and an ineffective quencher of O^* atoms, the deactivation rate constants are $(1.5\pm0.5)\times10^{-10}$ cm^3/s [16] and $(1.8\pm0.26)\times10^{-14}$ cm^3/s [1,17], respectively. Thus, in the measurements of this kind the formation of Cl^* was of no importance.

Note that this determination is the only absolute measurement of rate constants in the present Letter. In the subsequent text, only relative rate data are presented.

3.3. Relative rates for $O^* + XCl \rightarrow Cl + OX$ reactions

The method for determination of the ratios between k_{ia} and k_i $(i=1,2)$ has been described previously [6,7]. Briefly, in the experiments of this kind the $O_3/XCl/SF_6/He$ gas mixture was photolyzed; [XCl] was varied, all other concentrations were kept constant; the maximum amplitude of Cl signal was measured. Cl atoms are produced only by the $O^* +$ XCl reaction. All secondary radical–radical reactions are negligible over the time scale of the present experiments. SF_6 was added in the gas mixture to deactivate Cl^*. The LMR signal of Cl atoms reached a maximum at several microseconds and decayed slowly over several milliseconds.

The maximum Cl concentration after the complete deactivation of O^* is given by the expression

$$[Cl]_{max} = \frac{k_{ia}[XCl]}{\boldsymbol{k}(XCl, O_3, SF_6, He)}[O^*]_0, \qquad (5)$$

where i is equal 1 or 2 for X = H or D, respectively, $[O^*]_0$ is the initial concentration of O^* atoms. Expression (5) reduces to

$$S_{Cl} = \frac{A_i[XCl]}{B_i + [XCl]}, \qquad (6)$$

where parameters A_i and B_i are defined as

$$A_i = (k_{ia}/k_i)[O^*]_0/\Theta, \qquad (7)$$

$$B_i = \boldsymbol{k}(O_3, SF_6, He)/k_i. \qquad (8)$$

Here the Θ factor converts the chlorine atom concentration into LMR signal amplitude, $\Theta[Cl]_{max} = S_{Cl}$.

Rearrangement of Eqs. (7) and (8) gives

$$k_{1a}/k_{2a} = (A_1/B_1)/(A_2/B_2), \qquad (9)$$

$$(k_{1a}/k_1)/(k_{2a}/k_2) = A_1/A_2, \qquad (10)$$

$$k_1/k_2 = B_1/B_2. \qquad (11)$$

Plots of S_{Cl} vs. [XCl] were obtained experimentally. A least-squares fit of the plots by expression (6) yields the A_i and B_i parameters. Since all the values in the right-hand side of relationships (9)–(11) are determined from experiment, we determine all ratios between k_{ia} and k_i rates as listed in Table 2. Note that k_1/k_2 and k_{1a}/k_1 ratios are known, see Section 3.2 and Refs. [6,18], respectively; hence only one new ratio k_{2a}/k_2 was obtained.

The most useful is relation (10) since it requires only the $[XCl] \gg [O_3]$ condition and does not require accurate measurements of XCl flows. Fig. 2 shows examples of the variations of S_{Cl} with [XCl]. From the variations the $(k_{1a}/k_1)/(k_{2a}/k_2)$ ratio have been obtained. It was found to be close to unity (~ 0.86).

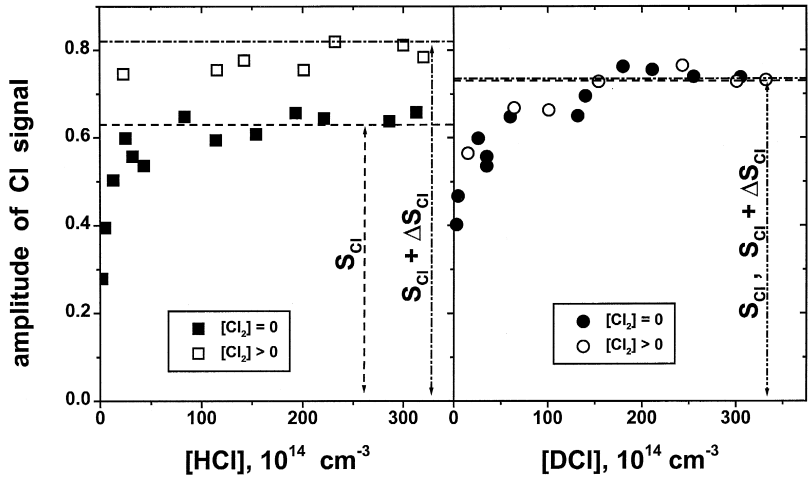

Fig. 2. Examples of the variations of the Cl atom signal amplitude with [HCl] and [DCl]. The amplitudes S_{Cl} and ΔS_{Cl} correspond to the reactions $O(^1D) + HCl$ and $H + Cl_2$, respectively. The relative rate constants were obtained from the limiting values ($[XCl] \to \infty$) of the amplitudes (Eq. (12)).

3.4. Relative rates for $O^* + XF \to F + OX$ reactions

The method for determination of the ratios between k_{ia} and k_i $(i = 3, 4)$ has been described previously [7]. It is similar to that described in Section 3.3 for determination k_{1a} and k_{2a} except that XCl is replaced by XF and FO radicals are monitored instead of Cl atoms. The FO radicals are produced in reaction of F atoms with O_3. The maximum amplitude of the signal was measured.

Plots of S_{FO} vs. [XF] have been obtained. In experiments with excess of [XF] the amplitude of FO signals was equal for HF and DF; hence the ratio $(k_{3a}/k_3)/(k_{4a}/k_4) \approx 1$ was obtained. The ratio k_3/k_4 was not established because of difficulties with accurate measurement of XF flow.

3.5. Relative rates for $O^* + XCl \to X + ClO$ reactions

The present method for determination of the ratios k_{1b}/k_{1a} and k_{2b}/k_{2a} has not been used previously. In the experiments of this kind the $O_3/XCl/SF_6/(Cl_2)/He$ gas mixture was photolyzed. [XCl] was varied, all other concentrations were kept constant. The information was obtained from comparison of the maximum amplitude of Cl signal measured without Cl_2 and in presence Cl_2; these amplitudes are denoted S_{Cl} and $S_{Cl} + \Delta S_{Cl}$, respectively.

The condition $[XCl] \gg [Cl_2] \gg [O_3]$ was obeyed. Since $k_{XCl} \approx k_{Cl_2} \approx k_{O_3}$, O^* atoms were deactivated mainly by XCl. Since the rates of reactions of H with Cl_2 and O_3 are close, in the presence of Cl_2 chemically produced H atoms interacted mainly with Cl_2 to produce Cl atoms. In other words, molecular chlorine converts X atoms to Cl atoms. Note that the reaction of OH with Cl_2 is slow (8×10^{-14} cm^3/s [22]) and therefore it can be neglected. Hence the production of Cl atoms is due both to the $O^* + XCl$ and $H + Cl_2$ reactions. SF_6 was added in the gas mixture to deactivate Cl^*.

The amplitude of the LMR signal of Cl atoms is given by Eqs. (5) and (6), but in the presence of Cl_2 k_{ia} is substituted by $(k_{ia} + k_{ib})$, here $i = 1, 2$. Hence the ratio of the amplitudes is given by

$$\Delta S_{Cl}/S_{Cl} = k_{ib}/k_{ia}. \qquad (12)$$

This relation was used to determine the k_{ib}/k_{ia} ratios, see Fig. 2. For $O^* + HCl$, this ratio was measured to be $k_{1b}/k_1 = 0.28 \pm 0.05$, in agreement with the literature. For $O^* + DCl$, the addition of Cl_2 had no effect upon the amplitude of the Cl atoms signal. Hence only upper limit for the ratio was estimated, $k_{2b}/k_2 < 0.04$.

3.6. Formation of $Cl(^2P_{1/2})$

In the experiments of this kind the $O_3/XCl/SF_6/He$ gas mixture was photolyzed. $[SF_6]$ was varied, all concentrations were kept constant. the maximum amplitude of Cl signal was measured.

Note that the LMR signal of Cl is proportional to the difference $[Cl(X)] - (f^*/f)[Cl^*]$, here f and f^* are the statistical populations of the sublevels probed relative to the total populations of the ground $^2P_{3/2}$ and excited $^2P_{1/2}$ states, respectively ($f = 1/16$, $f^* = 1/8$; $Cl(X) \equiv Cl(^2P_{3/2})$. Temporal profiles of Cl signal were simulated by a simple kinetics scheme [6]. In the scheme the decay of O^* atoms, the formation and deactivation of Cl^* atoms are taken into account. Following this scheme, the temporal profiles are described by the kinetic expression for a two-step process:

$$[Cl(X)] - 2[Cl^*] = \tau k_{ia}[O^*]_0[XCl]\left[1 - \exp(-t/\tau) + \frac{3\beta_i}{1 - k^*\tau}\{\exp(-t/\tau) - \exp(-k^* t)\}\right], \quad (13)$$

where τ is the decay time of O^* atoms and k^* is the pseudo-first-order rate coefficient for the deactivation of Cl^* by SF_6, XCl, O_3, and He.

Rearrangement of Eq. (13) gives

$$S^*_{Cl}/S_{Cl} = 1 - 3\beta_i, \quad (14)$$

where S^*_{Cl} and S_{Cl} are the maximum amplitudes of the LMR signal measured without SF_6 ($\tau k^* \ll 1$) and in excess of SF_6 ($k^* \to \infty$), respectively. This relation was employed for the data analysis. The β_1 and β_2 values were obtained from this analysis as 0.19 ± 0.04 and 0.20 ± 0.04 ($\pm 2\sigma$), respectively.

In our previous study we analysed the time of signal rise τ using Eq. (13) [6]. The best agreement between the experimental $1/\tau$ vs. $[SF_6]$ data and simulations was obtained at $\beta_1 = (0.10 \pm 0.04)$, in poor agreement with the value obtained in the present study. It seems likely that the present results are more reliable since: (1) in such experiments the rise time is not far from the time resolution of the LMR spectrometer and this fact was not taken into account; and (2) the rate constant for the deactivation process $Cl^* + SF_6 \to Cl(X) + SF_6$ is known with significant uncertainty [16,23]. Note that the present method for determination of the β_i values does not require a precise value for this rate constant.

4. Discussion

4.1. On the mechanism for $O^* + XCl \to X + ClO$ reactions

The large isotope effect on the the channel branching ratio $[X + ClO]/[Cl + OX]$ was first found by Matsumi et al. [9] We have now extended the study of Matsumi et al. and report here probabilities of all three channels and the deactivation rates for $O^* + XCl$ processes. From Table 2 it can be seen that the $[D + ClO]/[Cl + OD]$ ratio is equal to 0.09 ± 0.02 at average collisional energies of 7.7 kcal/mol [9], and it is < 0.04 at $T = 300$ K. Hence the ratio depends on collisional energy; the higher the energy, the higher the ratio.

There is a discussion in the literature concerning the pathway for the $O^* + HCl \to H + ClO$ reaction channel. It may be either via the ground state $X\,^1A'$ $HOCl/HClO$ energy surface or via the first excited singlet $^1A''$ HOCl surface [24], see adiabatic correlation diagram at Fig. 3. The angular and velocity distribution of the ClO product from the reaction has been measured by Balucani et al. [21]. The observation of almost backward-forward symmetric distribution led to the conclusion that reaction (1b) most likely proceeds via a long-lived complex. That is, via the ground state $X\,^1A'$ surface since there is no

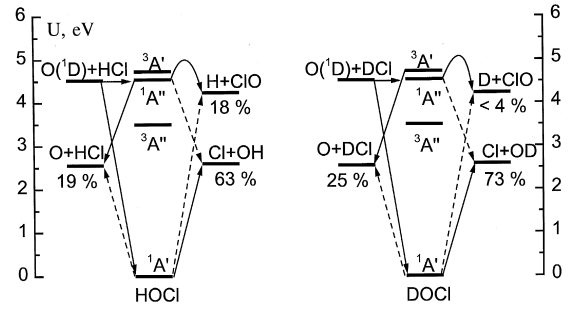

Fig. 3. Energy level diagrams showing possible reaction pathways and their probabilities for $O^* + HCl$ and $O^* + DCl$ systems.

significant potential well on the excited $^1A''$ surface. However, there are two facts which lead to the opposite conclusion. First, the large fraction ($\sim 43\%$) of H + ClO product energy released into translation indicates the existence of a barrier in the exit channel [21]. There is a small barrier for hydrogen removal HOCl → H + ClO on the excited $^1A''$ surface [24], and there is no barrier on the ground state $X\,^1A'$ surface [5]. Second, the large isotope effect on the channel branching ratios [X + ClO]/[Cl + OX] observed both in the present study and by Matsumi et al. cannot be reproduced by statistical theory of unimolecular decay [9]. Hence, the pathway leading to the X + ClO via XOCl($X\,^1A'$) complex is in doubt. Note that the [X + ClO]/[Cl + OX] ratios may be explained if reactions (1b) and (2b) proceed via the barrier on the excited $^1A''$ surface, if the difference in zero-point energy between HCl and DCl is taken into account.

The third argument is brought forward in the present study. The common statement is that reaction (1a) proceeds via the ground surface [3–5]. If reaction (1b) proceeds via the ground surface also, channels (1a) and (1b) must compete. Hence, the strong decrease of X + ClO channel probability in the deuterated case must lead to a strong increase of the Cl + OX channel probability. This increase was not observed, hence it is tempting to think that reactions (1a) and (1b) proceed via different surfaces.

4.2. On the formation of Cl($^2P_{1/2}$)

The probabilities of Cl^* formation in reactions (1a) and (2a) were measured previously by Matsumi et al. [9], using (2 + 1) REMPI technique at average collisional energies of 7.6 and 7.7 kcal/mol, respectively. The values $\beta_1 = 0.166 \pm 0.04$ and $\beta_2 = 0.153 \pm 0.03$ have been obtained. In the current study the values $\beta_1 = 0.19 \pm 0.04$, $\beta_2 = 0.20 \pm 0.04$ are determined at room temperature. The agreement between the results of these two studies is rather well, although the collisional conditions are quite different.

It was proposed that the excitation of Cl atoms proceeds via *R–E* energy transfer in the exit channel region at large distances between OX and Cl [6,9]. Our estimate based on long-range multipole–quadrupole interaction gives a reasonably good agreement with experimental results for the reaction of O^* with HCl, but the calculated β_2 value is ~ 2.5 times lower than the experimental one [8]. We feel that further improvement of the model will not give the relation $\beta_1 \approx \beta_2$ observed experimentally because of the large difference in the rotational constants of OH and OD. Hence, the mechanism of the formation of Cl^* remains unclear.

5. Summary

The main new results obtained in the present study may be expressed, within experimental error, as $k_1 = k_2$, $k_{1a} \approx k_{2a}$, $k_{1b} \gg k_{2b}$, and $k_{3a} = k_{4a}$. That is, the H ↔ D isotopic substitution does not change the rate constant for total deactivation of O^* by XCl and the probability of the main Cl + OX channel; it changes the relative importance of ClO + X and O + XCl channels. Also, there is no isotope effect on the channel branching ratios for deactivation of O^* by XF.

Acknowledgements

This work was supported by the Russian Foundation for Basic Research through Grant 97-03-33649a.

References

[1] A.R. Ravishankara, S. Solomon, A.A. Turnipseed, R.F. Warren, Science 259 (1993) 194.
[2] K. Schofield, J. Photochem. 9 (1978) 55.
[3] R. Schinke, J. Chem. Phys. 80 (1984) 5510.
[4] C.R. Park, J.R. Wiesenfeld, Chem. Phys. Lett. 163 (1989) 230.
[5] M.L. Hernandez, C. Redondo, A. Lagana, G.O. Aspuru, M. Rosi, A. Sgamellotti, J. Chem. Phys. 105 (1996) 2710.
[6] A.I. Chichinin, J. Chem. Phys. 106 (1997) 1057.
[7] V.I. Sorokin, N.P. Gritsan, A.I. Chichinin, J. Chem. Phys. 108 (1998) 8995.
[8] A.I. Chichinin, Chem. Phys. Rep. 16 (1996) 635.
[9] Y. Matsumi, K. Tonokura, M. Kawasaki, K. Tsuji, K. Obi, J. Chem. Phys. 98 (1993) 8330.
[10] M. Dagenais, J.W.C. Johns, A.R.W. McKellar, Can. J. Phys. 54 (1976) 1438.
[11] V.R. Braun, L.N. Krasnoperov, V.N. Panfilov, Opt. Spectrosk. 52 (1982) 719.
[12] A.R.W. McKellar, Can. J. Phys. 57 (1979) 2106.

[13] A.I. Chichinin, L.N. Krasnoperov, Chem. Phys. 143 (1990) 281.
[14] F.M. Rapoport, A.A. Ilyinskaya, Laboratory Methods of Pure Gases Synthesis, GosKhimIzdat, Moscow, 1963.
[15] W.B. DeMore, S.P. Sander, C.J. Howard, A.R. Ravishankara, D.M. Golden, C.E. Kolb, R.F. Hampson, M.J. Kurylo, M.J. Molina, Chemical Kinetics and Photochemical Data for Use in Stratospheric Modeling, vol. 11, NASA, Calif. Inst. Technol., Pasadena, CA, 1994, JPL Publ. 94-26.
[16] S.A. Sotnichenko, V.Ch. Bokun, A.I. Nadkhin, Chem. Phys. Lett. 153 (1988) 560.
[17] J.A. Davidson, C.M. Sadowski, H.I. Schiff, G.E. Streit, C.J. Howard, D.A. Jennings, A.L. Schmeltekopf, J. Chem. Phys. 64 (1976) 57.
[18] P.H. Wine, J.R. Wells, A.R. Ravishankara, J. Chem. Phys. 84 (1986) 1349.
[19] J.A. Davidson, H.I. Shiff, G.E. Steit, J.R. McAfee, A.L. Schmeltekopf, C.J. Howard, J. Chem. Phys. 67 (1977) 5021.
[20] E.J. Kruus, B.I. Niefer, J.J. Sloan, J. Chem. Phys. 88 (1988) 985.
[21] N. Balucani, L. Beneventi, P. Casavecchia, G.G. Volpi, Chem. Phys. Lett. 180 (1991) 34.
[22] R.B. Boodaghians, I.W. Hall, R.P. Wayne, J. Chem. Soc., Perkin Trans. 2 83 (1987) 529.
[23] A.I. Chichinin, Time-resolved LMR study of deactivation of Cl (2P1/2), J. Chem. Phys. (in press).
[24] P.J. Bruna, G. Hirsch, S.D. Peyerimhoff, R.J. Buenker, Can. J. Phys. 57 (1979) 1839.